Unmanned Target Vehicle Navigation and Path Planning Using Improved Ant Colony Optimization Algorithm Combined with GPS/BDS

Rongli Cai
School of Optoelectronic Engineering, Xi'an Technological University, China
RongliCai1990@outlook.com

Abstract: *With the rise of technology, mobile unmanned target vehicles have become common in military training. These vehicles carry shooting targets, offering troops mobile targets for shooting practice and enhancing simulated training effectiveness. However, in complex terrains, the movement path of unmanned vehicles falls short of achieving desired results. Path planning for unmanned target vehicles has therefore gained importance. To optimize their movement and enhance military training, a robust adaptive positioning algorithm based on Global Positioning System/Bei Dou System (GPS/BDS) technology is proposed. This algorithm ensures precise positioning and trajectory prediction. Additionally, the Ant Colony Optimization (ACO) algorithm is improved by considering heuristic factors and defining restricted regions, optimizing the trajectory. Simulation experiments demonstrate high-precision navigation and positioning, reducing signal propagation time and improving smoothness and directionality. The path length approximates the optimal path with minimal error. Comparative experiments confirm the algorithm's accuracy and efficiency in planning paths with speed, fewer turns, and improved smoothness. This optimization helps unmanned target vehicles enhance their trajectories and improve military training effectiveness.*

Keywords: *Ant colony, BDS, GPS, path planning, unmanned target vehicle.*

Received February 3, 2024; accepted June 23, 2024
https://doi.org/10.34028/iajit/21/4/5

1. Introduction

With the continuous development of science and technology and the continuous improvement of military training requirements, the conventional fixed target training method is being phased out. Unmanned target vehicles that can move independently are suitable for mobile target training and have been widely used in the military field. Unmanned target vehicles require the assistance of navigation systems to move toward the target. The positioning and navigation technology of unmanned target vehicles mainly relies on Global Positioning System (GPS) and Bei Dou System (BDS) [12, 16, 21]. However, due to the influence of signal occlusion, multipath effect and other factors, the positioning accuracy may be limited. The combination of GPS/BDS positioning method and unmanned target vehicle positioning and navigation is studied to improve the positioning accuracy and reliability of unmanned target vehicle. By combining various positioning techniques, the unmanned target vehicle can more precisely identify and navigate towards the desired location. In addition, the premise of autonomous movement of mobile unmanned target vehicles is that they have the ability to plan paths, so the selection of path search algorithms needs to be carefully considered.

However, the existing algorithms have the problems of high computational complexity, easy to fall into the local optimal solution, and insufficient processing of terrain constraints. Therefore, to address existing deficiencies in GPS/BDS navigation and positioning algorithms, a sturdy adaptable positioning algorithm utilizing GPS/BDS pseudo range Doppler observations is proposed. This will enhance both the original method and its accuracy and autonomous motion ability [20, 26]. Ant colony algorithm has the advantages of strong robustness. However, the traditional ant colony algorithm may fall into the problem of local optimal solution in path search, so this study introduces additional information to guide ant colony search, and constrains it by heuristic factor weights and setting band gap to improve its search accuracy. Based on this situation, the study proposes unmanned target vehicle navigation and path planning using improved Ant Colony Optimization (ACO) algorithm combined with GPS/BDS. There are three innovative points in this paper: Firstly, an unmanned target vehicle positioning and navigation method is proposed that combines GPS/BDS positioning. This method improves the accuracy and reliability of positioning. Second, the paper introduces a robust adaptive localization algorithm based on GPS/BDS pseudo range Doppler observations. This algorithm establishes a suitable random model based on the GPS/BDS dual system to meet the requirements of real-time dynamic data processing; Establish a detection method based on pseudo range single difference to eliminate the

influence of gross errors in GPS/BDS observation errors. Additionally, it constructs an adaptive factor based on a one-step robust solution to dynamic model errors for achieving robust adaptation. This can introduce more exploration into the search process, avoid falling into the local optimal solution, and improve the optimization effect of the path.

2. Related Work

Path optimization has always been a hot topic in road planning research. Numerous scholars have explored path optimization methods from multiple perspectives and perspectives. Xu *et al*. [25] proposed an improved artificial potential field model to improve the performance of the artificial potential field model in path planning problems. This model discards the local minimum of traditional models while avoiding obstacles, and uses the repulsive potential surface of local optimization to obtain the optimal path. This experiment illustrates that the improved artificial potential field method can quickly adapt to changing environments and efficiently plan collision-free paths. To optimize the driving route of vehicles in path tracking and reduce vehicle collision accidents, Lin *et al.* [14] proposed a model curve fitting method combining artificial potential fields. The approach utilizes quadratic programming to define the rolling curve of the vehicle, partially restricts the optimization process of the path, and includes the front and vehicle waypoints in the path planning. Simulation experiments have shown that the model curve fitting method can plan safe driving routes in the presence of obstacles and has high efficiency in finding traffic paths. To optimize the motion path of vehicle-like mobile robot, Sathiya *et al.* [17] proposed an improved multi-objective Particle Swarm Optimization (PSO) model with fuzzy enhancement, and used the fuzzy reasoning system to avoid obstacles. And in the experiment of vehicle like robots, robot dynamics and system constraints are used as parameter variables to ensure the degree of freedom for path exploration. The simulation results showcase that the path planned by the improved PSO method has high security and does not collide with obstacles, so it has application value. To optimize the transportation route of radioactive materials and reduce transportation risks and costs, Tao *et al.* [19] proposed a comprehensive path planning method that combines risk awareness. This method considers risk, time, and economic cost, culminating in the creation of a probabilistic safety assessment model and grey correlation analysis model. Planning indicators are added to determine the path. The experimental results indicate that the comprehensive path planning method can effectively reduce transportation risks and costs. To optimize the global movement path of unmanned vehicles, scholars such as Cui *et al.* [7] combined an improved ACO model to design and optimize a global path planning model. This model determines the level of pheromone distribution by incorporating the positional relationship of each mobile node. Meanwhile, it uses the weight factor to speed up the pheromone update and ensure the number of pheromone to prevent premature convergence. This ultimately ensures the adaptability of the model to the experimental environment and can effectively reduce the cost of mobile control. Cheng *et al.* [6] proposed the AMENet model to address the complexity and uncertainty of autonomous and robot navigation trajectories, utilizing feature extraction and attention mechanisms in encoding. Specifically, AMENet includes two main components: a map encoder and a trajectory encoder. Map encoders are used to extract map features, while trajectory encoders fuse trajectory information with map features. Through the attention mechanism, AMENet can adaptively capture map related information in trajectories. Finally, by using the features obtained by the encoder, AMENet can make accurate trajectory prediction. Abdulla *et al.* [1] increased the prediction accuracy of moving object paths and proposed a HarmonyMoves unified prediction method. This method combines multiple prediction models and utilizes harmonious search algorithms to improve the accuracy of predictions. By integrating the prediction results of multiple models, HarmonyMoves can better predict the future path of moving objects. Chen *et al.* [5] aim to optimize the flow of urban traffic by reducing congestion and improving transportation efficiency. They introduced dynamic path selection algorithms and considered the travel needs of users and the state of the transportation network. Through intelligent decision-making and allocation mechanisms, they adjusted the paths of shared vehicles, thereby improving the overall efficiency of the transportation system. Through simulation experiments and numerical analysis, it has been proven that this dynamic path optimization strategy can effectively alleviate urban traffic congestion.

ACO, as a probabilistic model, is widely used in global optimization research. Whether it is combinatorial optimization problems such as traveling salesman problems, vehicle routing problems, or continuous optimization problems, ACO can play a powerful role. By continuously adjusting the behavior rules and parameter settings of ants, the ACO algorithm can find high-quality solutions in various complex scenarios. To solve the problem that the proportional integral differential controller in the nonlinear system does not respond well to the changes of motor system parameters, Mahfoud *et al.* [15] proposed a strategy of combining ACO models. This approach enhances the gain of proportional integral differentiation through utilization of integral squared error as a cost function, and is applied to both sides of a doubly fed asynchronous motor. The research results indicate that the combined ACO model can ensure the effectiveness

of proportional integral differential under direct torque control and improve the global performance of the system. To improve traditional liquid sensors, Fang *et al.* [9] the ACO model for numerical optimization of the structure of artificial magnetic conductors. Then, a broadband antenna is introduced to design a liquid sensor, and the liquid sample is injected directly into the internal structure of the sensor. Simulation experiments have shown that the ACO model can reduce the manufacturing cost and response time consumption of liquid sensors, and improve the structural optimization of sensors. To help alleviate network hotspot issues through data collection strategies based on mobile beacons, Boyineni *et al.* [3] introduced ACO into the data collected by mobile beacons to improve network energy efficiency and traffic by reducing network speed latency. Then the researchers used ACO to simultaneously select network relay nodes and traffic paths, and adopted a virtual relay node selection strategy to avoid redundant data exchange. Ultimately, it can reduce network burden and usage pressure. To optimize the distribution route of low-carbon fresh cold chain logistics, Wu *et al.* [23] proposed a distribution model with the ratio of minimum total cost and maximum satisfaction as the objective function. The model takes into account various factors, including customer satisfaction and cost. It employs the improved algorithm and ant colony algorithm to solve the problem. The results show that the improved ant colony algorithm can efficiently and accurately find the optimal solution for the single objective low-carbon fresh agricultural products cold chain logistics distribution model. To improve the accuracy and freedom of big data anomaly detection methods, Xu [24] proposed a hybrid big data segmentation anomaly detection model combined with ACO. This model redefines the number of network node neighbors, and regards the high concentration pheromone position obtained from the ant colony model as an abnormal position to introduce the security status value, and finally completes the big data detection. Simulation experiments showed that the improved detection method has a high level of accuracy, superior positioning flexibility, and efficient system performance.

In conclusion, many experts and scholars have solved the global optimization problem through ACO algorithm, and proposed various planning models to optimize the mobile path and reduce the mobile cost. However, traditional ACO algorithms are also prone to problems such as local optima and poor convergence in the path planning process. Additionally, path planning of unmanned target vehicles is necessary for military training, which demands both confidentiality and precision. Therefore, it is necessary to improve the traditional planning model to improve the planning accuracy. Therefore, the study utilizes an improved ant colony model to combine the Global Positioning System (GPS) and the Beidou Navigation Satellite System (BDS) to design an unmanned target vehicle navigation and path planning model, hoping to provide support for the optimization of the moving path of unmanned target vehicles, improve the accuracy and effectiveness of path planning, and ultimately enhance the effectiveness of military training.

3. Improve the Design of Path Planning Model for ACO Combined with GPS/BDS

3.1. Design of GPS/BDS Combined Positioning Model Based on KF Model

To optimize the path of an unmanned target vehicle, it is first necessary to develop a positioning model to determine the position and motion state of the unmanned target vehicle. Satellite positioning is a commonly used method for locating ground positions. The satellite positioning system mainly consists of navigation satellites in orbit, ground receivers, and user-carried navigation devices [2, 13]. The basic principle of a positioning system is to calculate the distance between the positioning satellite and the ground signal receiving equipment. This distance data is then integrated from multiple satellites to determine the receiver's position. Then, the pseudo range distance is obtained by multiplying the time the user's device receives the satellite signal by the speed of light. Finally, the true distance between the user and the positioning satellite is calculated utilizing the pseudo distance [11, 18]. The combination of GPS and BDS positioning utilizes signals from both systems to improve the accuracy and reliability of positioning. By receiving signals from both GPS and BDS simultaneously, the receiver can obtain more satellite information, thereby improving positioning accuracy and enhancing the robustness of the system to some extent, as even if one system signal is disturbed or unavailable, the other system can still provide positioning information. In order to realize the combined positioning of GPS and BDS, a GNSS navigation receiver that can receive both GPS and BDS signals is selected. GNSS receivers collect signals from GPS and BDS satellites, convert them into position and time data, then decode and compute the data to generate precise location information. Finally, the PSO combined positioning algorithm is used to fuse the measurement data of GPS and BDS to obtain the final position solution result [10, 22]. Combining the pseudo-range observations from both GPS and BDS systems for positioning solution can improve the accuracy and reliability of positioning. The combined GPS/BDS positioning system is shown in Figure 1.

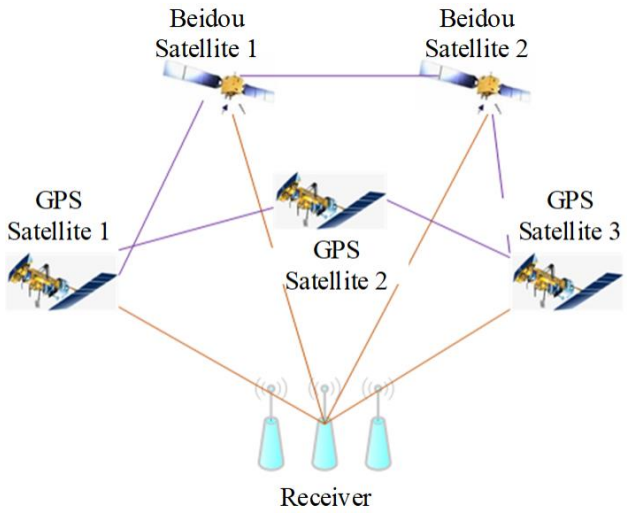

Figure 1. Combined GPS/BDS positioning system.

The receiver in Figure 1 can show the signal reception time, satellite ephemeris and Doppler and other satellite information of the combined GPS/BDS positioning system. The GPS/BDS navigation and positioning model is divided into two parts: the functional model and the stochastic model. The functional model describes the mathematical function relationship between the position observation vectors and the user's state vectors, while the stochastic model describes the position observation vectors and the statistical correlation between them. The function model is constructed by unifying the spatial and temporal datums of GPS/BDS, using the WGS84 coordinate system for GPS and the CGCS2000 coordinate system for BDS. Thereafter, individual satellite navigation systems' observation equations are introduced, as demonstrated in Equation (1).

$$y = AX + \xi \tag{1}$$

In Equation (1), is the -dimensional pseudo-distance observation vector; is the coefficient matrix; is the pseudo-distance observation parameter; and is the observation error. The formula for determining single-point location using pseudorange is shown in Equation (2).

$$P_A^i = \sqrt{(X^i - x)^2 + (Y^i - y)^2 + (Z^i - z)^2} + cdt - c\sigma t^i - d_{ion}^i + \varepsilon \tag{2}$$

In the Equation (2), is the pseudo-distance between occupied stars; is the number of satellites; is the coordinate of the station; is the coordinate of the satellite; is the vacuum speed of light; is the clock difference of the satellite; is the clock difference of the receiver; is the ionisation delay; is the delay in the troposphere; and is the modelling error and observation noise. This equation is generally used for single-point positioning of a single system using pseudo-ranging. However, for the combined positioning of two systems, it is necessary to combine the positioning according to the basic equations, and the joint levelling is required to obtain the optimal solution. The observation equations after error correction are obtained according to the basic observation equations are shown in Equation (3).

$$p = p^A + \delta t^A - V_{ion}^A - V_{trop}^A \tag{3}$$

In Equation (3), is the combined GPS/BDS system; is the error-corrected pseudorange observation; is the error-corrected clock difference; is the improved ionospheric delay; and is the improved tropospheric delay. Then the pseudo-range observation equations of GPS and BDS navigation systems are combined. Then the Kalman filter method is used to solve the GPS/BDS navigation and positioning using the pseudo-range observations. Finally, the detected point's coordinates are obtained in both the WGS84 and CGCS2000 systems, with the ability to calculate distance errors for both GPS and BDS observation systems. Positioning using the combined GPS/BDS navigation system is bound to produce a certain amount of error, and the commonly used GPS/BDS navigation and positioning error detection method is IGGIII, the weights of which are calculated in Equation (4).

$$\bar{p}_i = \begin{cases} p_i & |v_i| \le c_o \\ p_i \dfrac{c_0}{|v_i|}\left(\dfrac{k_1 - |v_i|}{k_1 - k_0}\right) & c_o < |v_i| < c_1 \\ 0 & |v_i| \ge c_o \end{cases} \tag{4}$$

In Equation (4), is the normalised residual; is the equal weighting matrix; is the original weighting matrix; and is the reconciliation coefficients; and are constants. To navigate a moving object, it is necessary to predict the motion state of the object at the next moment. The first step is to determine the motion state of the object, for which there are two commonly used motion state models: the constant model and the constant acceleration model. After determining the object's motion state, then choose the appropriate filtering algorithm to update the predicted value of the object's position, so as to obtain more accurate physical position information. The above method can complete the positioning of the object, but there are still many shortcomings, the next will be for its shortcomings one by one to improve. Firstly, the traditional GPS/BDS combined positioning system is susceptible to various errors that can be resolved by enhancing the receiver's ability to receive satellite signals. In addition, it is known from the literature that the smaller the satellite altitude angle is, the greater the error propagated by the atmosphere is. Therefore, the carrier-to-noise ratio method and the satellite altitude angle method can be used to establish the GPS/BDS stochastic model, as shown in Equation (5).

$$\begin{cases} \sigma_i^2 = \dfrac{sigma_j^2}{\sin^2(E)} \\ C/N_0 = \dfrac{P_R}{N_0} \end{cases} \tag{5}$$

Equation (5) where is the altitude angle of the satellite; is the accuracy of each navigation system in the zenith direction; is the carrier to noise ratio; is the noise power spectral density; is the signal received power. The IGGIII method, on the other hand, addresses the problem of residuals of anomalous observations in the error detection of GPS/BDS navigation and positioning process, which leads to inaccurate error detection and diagnosis. The study proposes a two-step error detection model as an alternative. The two-step error detection model consists of a pseudo-detection model based on Equation (6).

$$\rho_k^s = R_k^s + c\delta t_k - c\delta t_k^s + \delta\rho_{k,trop}^s + \delta\rho_{k,ion}^s + \delta\rho_{k,rel}^s + \delta\rho_{k,sagnc}^s + \varepsilon_{p,k}^s \tag{6}$$

Equation (6) is a pseudo distance observation equation is; is the satellite number; is the speed of light; is the pseudo-distance observation; is the real distance from the receiver to the satellite; is the receiver clock difference; is the satellite clock difference; is the tropospheric delay error; is the ionospheric delay error; is the relativistic effect; and is the Earth's rotation error. In order to further reduce the influence of the coarseness of the GPS/BDS pseudorange observations on the navigation results, the coarseness is removed by using the antidifferential estimation. Addressing the issue that traditional filtering algorithms struggle to accurately update the predicted state value of moving objects at the next moment, the research proposes an open-window adaptive filtering algorithm. This methodology analyzes and obtains the discriminant statistic of the model error constructed in the face of redundant or insufficient observation values. The specific model is shown in Equation (7).

$$X_k = \phi_{k,k-1} X_{k-1} + W_k \tag{7}$$

In Equation (7), is the time corresponding to; the state of the dimension at time is; is the state matrix; is the State noise vector. The observation model of the moment is shown in Equation (8).

$$L_k = A_k X_k + \Delta_k \tag{8}$$

In Equation (8), is a-dimensional observation vector; is a-dimensional design matrix. The solution vector is shown in Equation (9).

$$\begin{cases} \hat{X}_k = \bar{X}_k + K_k (L_k - A_k \bar{X}_k) \\ \bar{X}_k = \phi_{k,k-1} \hat{X}_{k-1} \\ \Sigma_{\bar{X}_k} = (1 - K_k A_k \Sigma_{\hat{X}_k}) \\ K_k = \Sigma_{\hat{X}_k} A_k^T \left(A_k \Sigma_{\hat{X}_k} A_k^T + \Sigma_k \right)^{-1} \\ \Sigma_{\hat{X}_k} = \phi_{k,k-1} \Sigma_{\hat{X}_{k-1}} \phi_{k,k-1}^T + \Sigma_{W_k} \end{cases} \tag{9}$$

Based on Equations (7) to (9) the dynamic noise covariance matrix adaptive estimation can be introduced, see Equation (10).

$$\begin{aligned} \Sigma W &= \frac{1}{m} \sum_{i=0}^{m-1} V_{X_k - 1} V_{k-1}^T - \phi_{k,k-1} \\ &\Sigma_{\hat{X}_{k-1}} \phi^T{}_{k,k-1} + \Sigma_{\hat{X}_k} \end{aligned} \tag{10}$$

In Equation (10), is the state correction vector. The constructed adaptive factor can be based on the antidifferential solution to achieve the antidifferential adaptive and increase the positioning accuracy of the moving object dynamics model. The implementation flow of the antidivergence adaptive positioning based on GPS/BDS pseudorange Doppler observations is shown in Figure 2.

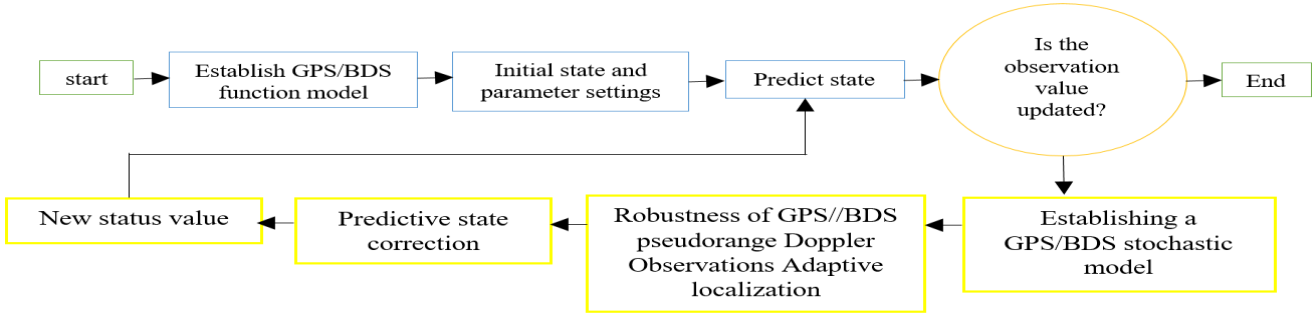

Figure 2. The positioning process of robust adaptive positioning algorithm based in GPS/BDS pseudo range Doppler observations.

As shown in Figure 2, the positioning process constructed in this study first constructs a GPS/BDS positioning system, predicts the satellite position based on the initial parameters received by the satellite signal, and then calculates the coordinate position of the target object through the GPS/BDS system pseudo range observation equation. During the calculation process, the use of the pseudo range single difference detection method is applied to handle gross errors generated in the calculation, resulting in a reduction of position calculation errors. The position of unmanned target aircraft is in a changing state, so a GPS/BDS random

model constructed using carrier to noise ratio and satellite altitude angle methods is used to achieve dynamic target position prediction. On the basis of robust computation, an adaptive factor is constructed using a windowed adaptive filtering algorithm to achieve robust adaptation.

3.2. Improving the Design of ACO Path Planning Model

After precise positioning of unmanned target vehicles through GPS/BDS combination, research needs to model the driving environment of unmanned target vehicles before conducting path planning. Environmental modeling requires simulating real situations and establishing models in abstract spaces. Therefore, it is necessary to use environmental modeling methods to abstract and transform the real environment. The grid modeling approach is frequently utilized in environmental modeling. Research on converting the initial position and endpoint targets of unmanned target vehicles into grids. Blank grids indicate passable areas, while colored grids indicate the presence of insurmountable obstacles. All positions of the constructed grid model are represented by coordinates, and planning the path of the unmanned target vehicle consists of planning a path that avoids obstacles from the starting position to the endpoint. The grid model constructed through research is shown in Figure 3.

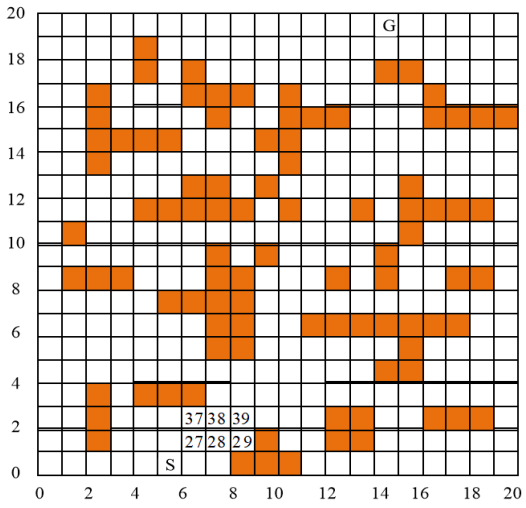

Figure 3. Basic construction of grid model.

In Figure 3, the letter S represents the starting position of the unmanned target vehicle; the letter G represents the endpoint position to which the unmanned target vehicle will move. Figure 4 shows that if the unmanned target vehicle moves to grid 38, the next position further after the elimination of the obstacle in the upper left corner. The horizontal and vertical coordinates of each grid are calculated as shown in Equation (11) [4, 8].

$$\begin{cases} x_i = \left[(i-1) \bmod N_h\right] + 1 \\ y_i = \left[\text{int}(i-1) N_h\right] + 1 \end{cases} \quad (11)$$

In Equation (11), N_h represents the number of grids per row; x_i represents the horizontal axis coordinate of the planned route; y_i represents the vertical axis coordinate of the planned route; Mod represents the remainder operation; int represents a rounding operation. After building the environment model, it is necessary to choose a path planning algorithm. The ACO algorithm can adjust the path search process through heuristic factors, making it highly adaptable. Therefore, the study adopts the ACO algorithm for global path planning. Figure 4 showcases the basic principle of the ACO algorithm.

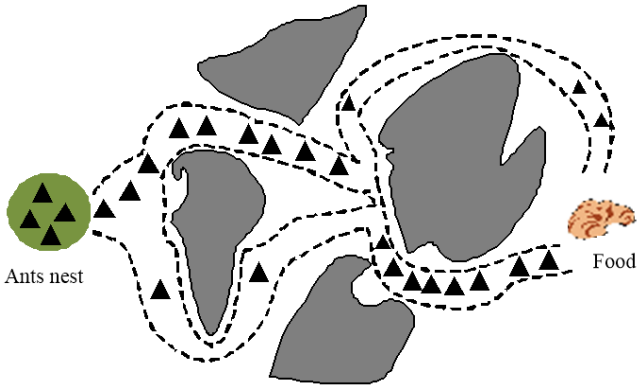

Figure 4. Basic framework of ACO.

The ACO algorithm is inspired by the foraging behavior of ants. The ACO algorithm realizes fast optimization through positive feedback information transmission and accumulation. Ants transmit signals and communicate with the whole population through pheromones secreted by the ants. The ants can find the shortest path thanks to the pheromone and the environment. As shown in Figure 5, there are the multiple paths between the ant nest and the food found by the ants. The ants that find food will transmit food signals by secreting pheromone to help other ants find food. Because the rate of pheromone volatilization is different for ants on different foraging routes, the shorter distance route has more pheromone; the route with longer distance has fewer pheromone. Other ants will also choose more routes of pheromone to obtain food more efficiently. However, when faced with multiple pheromone paths, ants must make their own path transfer. This prevents the ACO algorithm from getting trapped in a local optimal solution, as the transition probability function influences the path change of the algorithm. It is indicated in Equation (12).

$$p_{mn}(t) = \begin{cases} \dfrac{\left[\tau_{mn}(t)\right]^{\alpha} * \left[\eta_{mn}(t)\right]^{\beta}}{sum\left(\left[\tau_{ms}(t)\right]\right)^{\alpha} * \left[\eta_{ms}(t)\right]^{\beta}}, n \notin allow \\ 0, n \notin allow \end{cases} \quad (12)$$

In Equation (12), *allow* represents the set of ant access points; α refers to pheromone importance factor; β represents the heuristic function factor; $\tau_{mn}(t)$ is the pheromone concentration on the path from point m to point n; $\eta_{mn}(t)$ refers to the heuristic function, representing the ant's expectation from m to n; $\eta_{ms}(t)$ represents the heuristic function of ants to neighboring point s; $\tau_{ms}(t)$ refers to the pheromone concentration on the m-s path. It can be seen from Equation (12) that the pheromone concentration will greatly affect the path selection of the ants, so it is necessary to restrict the pheromone concentration of each path to prevent the initial path from attracting all ants due to a large number of pheromones. As a result, the pheromone concentration of each path is set as the maximum value of the pre-set pheromone concentration, while the smaller value of the heuristic factor weight is used. The research updates the pheromone concentration of the optimal path or the path of the iterative optimal solution, and analyzes the historical pheromone retention. The heuristic factor is often transformed into the reciprocal of adjacent paths in grid models, which is not conducive to improving the search efficiency. Therefore, the study divided the ant colony of the ACO algorithm into two groups and changed the weight parameters of the heuristic factor. The improved heuristic function can be designed, as shown in Equation (13).

$$\eta_{mn} = \frac{k_1}{d(n, goal)} + \frac{k_2}{d(m, n)} \tag{13}$$

In Equation (13), $d(m, n)$ refers to the length between adjacent grids; $d(n, goal)$ represents the remaining length from the current grid to the endpoint grid; k_1, k_2 refers to the weight coefficient used to improve the computational accuracy of the ACO algorithm. The setting conditions for the weight coefficient are shown in Equation (14).

$$\begin{cases} k_1 \gg k_2, ant \in group_1 \\ k_1 = 0, k_2 \gg k_1, ant \in group_2 \end{cases} \tag{14}$$

Ants will choose the path with the higher pheromone concentration when moving. However, this leads to congestion of a substantial number of ants in a particular path, causing a significant increase in pheromone concentration on that path. This loses the possibility of other ants finding a better solution. In Equation (14), the existence of G ant colony can make the pheromone not concentrated in a certain path, avoid the ACO algorithm convergence in advance, fall into the situation of local optimal solution, and meanwhile, do not deviate from the optimal path too much. The existence of E ant colony can improve the flexibility of path selection, prevent from delving into incorrect routes, and timely re plan routes. This ensures that the algorithm does not produce the worst possible solution. Ants will avoid the path chosen by other ants when searching the path. Only when the ants receive the pheromone representing the search for food will they enter the path of the search for food. Although individual ants may struggle to locate food sources, the collective search of the entire colony significantly enhances the efficiency of environmental information gathering. This can help the ant colony find food faster. The initial search path selection probability of ants is the same. Therefore, to increase the selection of the initial moving path of the ACO algorithm and help ACO algorithm to find other excellent paths that may appear, the study selects lower pheromone volatilization speed according to the pheromone concentration to reduce the pheromone difference. Then it improves the selection probability of the ant colony by increasing the total amount of pheromone of the optimal path. The pheromone updating process is illustrated in Equation (15).

$$\tau_{mn}(t+1) = (1-\rho)\tau_{mn}(t) + \Delta\tau_{mn}(t) + \frac{Q}{L_{best}} - \frac{Q}{L_{worst}} \tag{15}$$

In Equation (15), L_{best} refers to the optimal path length; L_{worst} refers to the worst path length; ρ is the pseudo distance. The study also considered the path planning problem in U-shaped obstacles, which are special obstacles like the letter U. The schematic diagram of U-shaped obstacles is shown in Figure 5.

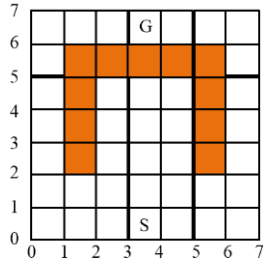

Figure 5. Schematic diagram of U-shaped obstacle.

Traditional ACO algorithms are prone to getting stuck in the concave areas in the middle of obstacles, leading to difficulty in finding the optimal path. The study aims to improve the ACO algorithm by recording the starting point of ant foraging in the set of restricted areas PA. When the ant chooses a path through Equation (12), it moves to node z. If there is no accessible area after that, that is, deep inside the U-shaped obstacle, node J is also considered as a non-accessible area and added to *PA*, and the ant moves back to the previous node v. If the node has no passable area except for node z, add v to *PA* and continue to fall back until there is a passable area. The principle of this improvement method is to record the ant movement node that accidentally enters the U-shaped obstacle and discard this path, and predict and set a prohibited passage zone in advance. Then it instructs the ant colony to find other paths in advance to avoid U-shaped obstacles, and repeatedly sets prohibited areas on the moving path until the ant colony reaches the endpoint.

In summary, the specific steps for ACO to combine GPS/BDS to achieve unmanned target vehicle

navigation and path planning are as follows: using GPS/BDS system to obtain real-time position and navigation information; Divide the navigation area into grids, each representing a possible location or intersection, determine the target position and starting position, and determine other constraints; Initialize the ant colony, where each ant has a certain number of pheromones, representing their preference for the path; Select the next moving grid based on its pheromone level, then update the pheromone based on the path length and efficiency, iteratively select the path until the stopping condition is reached, and finally output the optimal path.

4. Improvement of Unmanned Target Vehicle Navigation and Path Planning Model Effectiveness Testing

4.1. Precision Analysis of Unmanned Target Vehicle Navigation Model

To verify the accuracy of the improved GPS/BDS combined positioning model, a comparative experiment was conducted between the traditional least squares method combined with GPS/BDS combined positioning method and the Robust Adaptive Localization Algorithm for Pseudorange Doppler Observations combined with GPS/BDS combined positioning method. The maps used in the simulation experiment were obtained from open map datasets; The simulator uses MATLAB simulation software; The virtual satellite position and signal data come from GPS/BDS data simulators; The data of the unmanned target vehicle model is sourced from the GitHub platform; The experimental results are displayed on a Windows 10 computer equipped with an Intel i7-9500 CPU. The experimental results of simulated errors from the combination of the least squares method and GPS/BDS positioning are demonstrated in Figure 6.

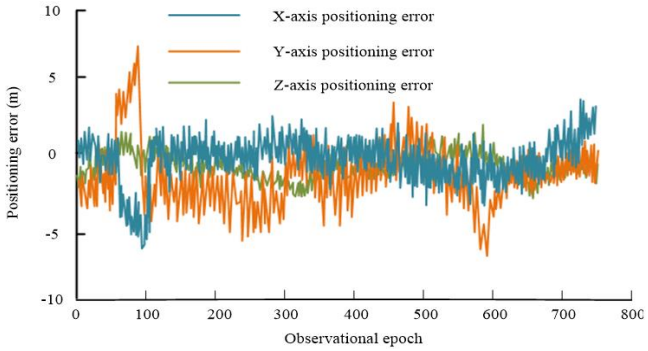

Figure 6. Least squares positioning error results.

Figure 6 showcases that the positioning coordinates of the unmanned target vehicle obtained by the least squares method maintain an error of about ± 7m in three-dimensional space, and can locate the position of the unmanned target vehicle through satellite signals. Nonetheless, the positioning axis exhibits fluctuation of around 7m with slow convergence speed, resulting in a relatively large overall fluctuation that contributes to an increase in linear error and a decrease in positioning accuracy. The error results of the robust adaptive localization algorithm for pseudorange doppler observations with GPS/BDS combination positioning are indicated in Figure 7.

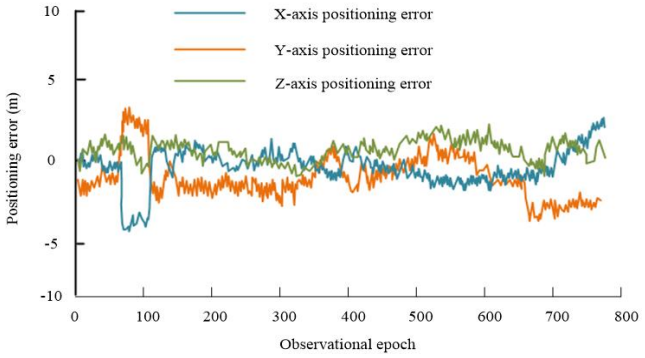

Figure 7. Robust adaptive localization algorithm based on GPS/BDS Pseudorange Doppler observations.

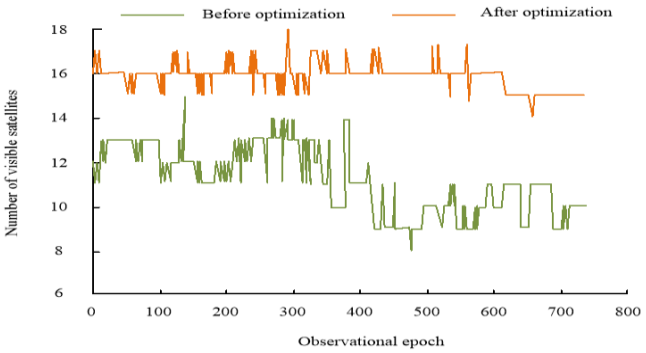

Figure 8. Number of visible satellites.

Figure 7 shows that the Robust Adaptive Localization Algorithm for Pseudorange Doppler Observations combined with GPS/BDS combined positioning model transmits the observation status at different times and corrects the position of the unmanned target vehicle based on the differences observed at different times. Therefore, the three-dimensional positioning error result remains within± 4m. Compared with the least-squares combined positioning method, the error line of the robust adaptive localization algorithm for pseudorange doppler observations combined GPS/BDS combined positioning model is smoother and more stable. This reduces the error caused by signal fluctuations, resulting in higher positioning accuracy. To further validate the effectiveness of the robust adaptive localization algorithm for pseudorange doppler observations combined with GPS/BDS combined positioning model, the study introduced positioning information from irregular environments into the observation model. The optimized positioning model was then compared to the pre-optimized model, and the results, including the number of satellites used, are shown in Figure 8.

Figure 8 indicates that the movement path of

unmanned target vehicles in complex road conditions is irregular, and noise data is difficult to obtain or even completely undetectable. Consequently, the optimized positioning model observes a relatively limited number of satellites, leading to imprecise location data. The optimized positioning model shows that the number of satellites has increased to 16 compared to before optimization, which is 6 more than before, indicating a relatively stable number of satellites. Therefore, the situation of positioning deviation is smaller, and the signal propagation time before and after model optimization is shown in Table 1.

Table 1 show cases that the signal propagation time before and after the optimization of the positioning model has a small change, but the overall signal propagation time after optimization is slightly smaller than before. A small decrease in signal propagation time can greatly enhance signal propagation efficiency and positioning accuracy during long-distance path planning. Therefore, the experiment verifies the accuracy of the optimized positioning model.

Table 1. Signal propagation time.

Experimental subjects	**GPS signal propagation time**		**Experimental subjects**	**BDS signal propagation time**	
Satellite number	Before optimization	After optimization	Satellite number	Before optimization	After optimization
5	0.0672	0.0668	2	0.1268	0.1277
10	0.0744	0.0743	4	0.1308	0.1302
15	0.0776	0.0775	6	0.1201	0.1201
25	0.0708	0.0709	8	0.1267	0.1260
30	0.0804	0.0804	10	0.1221	0.1224

To further demonstrate the superiority of the optimized GPS/BDS model, the positioning accuracy of GPS/Galileo model, GPS/GLONASS model, and GPS/BDS model were compared to simulate the positioning error values on the *X* and *Y* components of the unmanned vehicle within 1000 seconds. The results are shown in Figure 9.

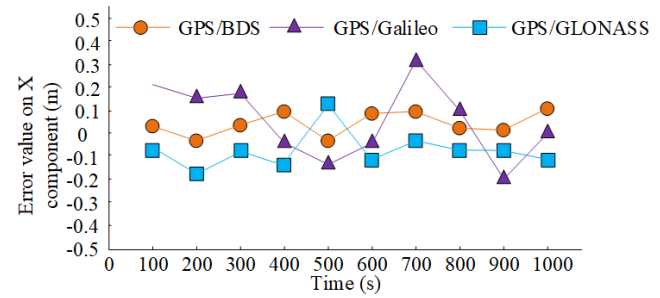

a) X component.

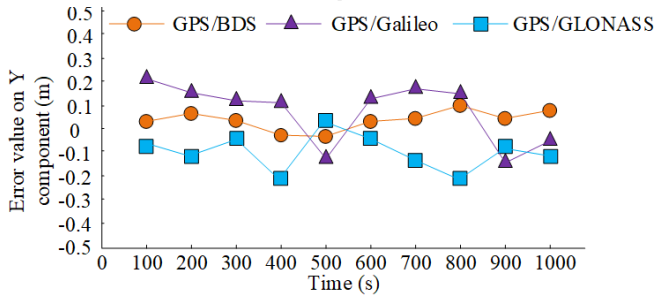

b) Y component.

Figure 9. Positioning error values of three systems on the X and Y components.

From Figure 9, it can be seen that the GPS/BDS model has relatively small errors in both the *X* and *Y* components, about ± 0.01m. However, the GPS/Galileo model and GPS/GLONASS model have relatively large errors and uneven fluctuations, indicating poor stability of these two positioning systems. Therefore, the optimized GPS/BDS combination model is used for unmanned positioning in the study.

4.2. Improved Path Planning Model Simulation Testing

The study focuses on using grid method for path planning in ant colony algorithm. The simulation matrix of grid method in Matlab mainly uses two data sets: 0 and 1, where 0 represents no obstacles and 1 represents obstacles. The grid design in the model is mainly based on squares or rectangles, and each area is sequentially designed for the grid interval. To represent the various positions of the grid, a continuous order was used, arranged from left to right and from top to bottom, forming a complete grid graph model. And set the parameters of the traditional ACO algorithm and the improved ACO algorithm as shown in Table 2.

Table 2. ACO algorithm parameter settings.

Parameter	**Traditional ACO algorithm**	**improves ACO algorithm**
Pheromone heuristic factor	0.3	0.4
Expected heuristic factor	0.2	0.4
Volatility coefficient of pheromones	0.8	0.7
The intensity of releasing pheromones	0.4	0.5
Algorithm parameters introduced	\	0.7
Adaptive factor	\	0.2
Maximum number of iterations number	500	500

Firstly, a robust adaptive positioning system based on GPS/BDS pseudo range Doppler observation is used to achieve precise positioning and navigation of the model, enabling it to accurately lock its position in complex terrain. Then, simulation experiments were conducted on the path planning under specific road conditions through grid modeling. The study initially evaluated the performance of the improved ACO path planning model when encountering U-shaped obstacles separately and compared it with traditional ACO models. The results of the U-shaped obstacle simulation test are shown in Figure 10.

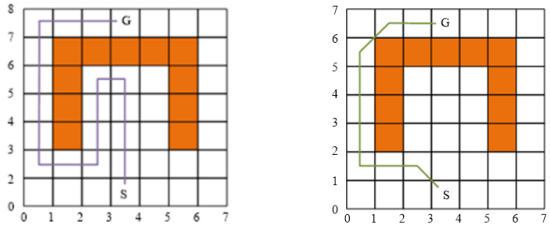

a) Traditional ant colony algorithm. b) Improved ant colony algorithm.

Figure 10. Number of visible satellites.

Figure 10 illustrates that traditional ACO path planning models often become caught in U-shaped obstacles, which leads to inadequate path planning solutions. The improved ACO path planning model can identify U-shaped obstacles in advance. It can self-correct in time before entering U-shaped obstacles, choose other paths to avoid obstacles, shorten the movement path, and achieve better optimization results. The study then conducted simulation experiments on the path planning model under different road conditions. The simulation experiments of two path planning models in the simple long-distance road condition M1 are shown in Figure 11.

Figure 11-a) shows the path planning of traditional ACO in simple road conditions; Figure 11-b) shows the path planning of improved ACO in simple road conditions. The above figure shows that under simple road conditions, both the traditional ACO path planning model and the improved ACO path planning model can find the optimal path. This indicates that the influence of heuristic factors on the ACO model is relatively small under simple road conditions. Figure 12 illustrates the simulation experimental outcomes of the path planning model in complex road conditions M1 and M2, which include U-shaped obstacles.

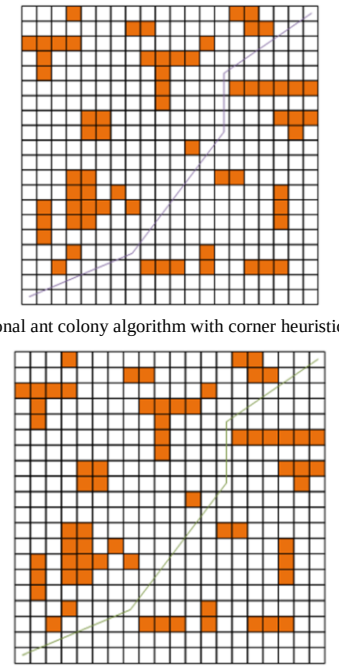

a) Traditional ant colony algorithm with corner heuristic function.

b) Improved ant colony algorithm.

Figure 11. Simple road condition simulation experiment results.

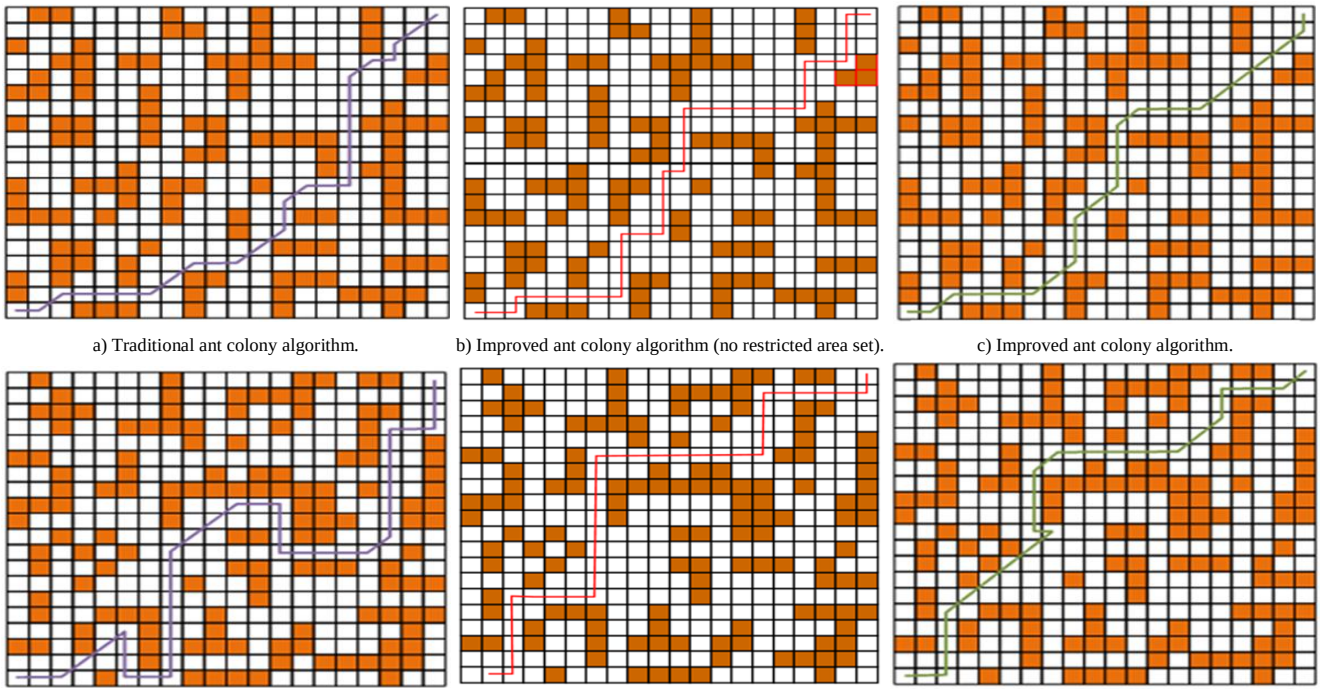

a) Traditional ant colony algorithm. b) Improved ant colony algorithm (no restricted area set). c) Improved ant colony algorithm.

d) Traditional ant colony algorithm with U-shaped disorder e) Traditional ant colony algorithm with U-shaped disorder (no restricted area set). f) Improved ant colony algorithm with U-shaped disorder.

Figure 12. Complex road condition simulation experiment results.

Figures 12-a), (b) and (c) showcase the path planning scenarios of two ACO algorithms in complex road conditions; Figures 12-d), (e) and (f) demonstrates the path planning of two ACO algorithms after the addition of U-shaped special obstacles. Figure 12 indicates that as the complexity of road conditions increases, especially conditions become more complex, particularly when special obstacles like U-shaped ones

are present, traditional ACO path planning models are susceptible to getting stuck in these obstacles. This will deviate from the optimal path, resulting in many unnecessary corners and increasing the length of the path. The improved path planning model can help unmanned target vehicles avoid poor paths in advance. The improved path planning model without adding prohibited zone settings only turns at right angles, and the moving path is still longer. The path planning model used in the study can choose the shortest theoretical path for movement. After organizing the data from several simulation experiments, it is shown in Table 3.

Table 3 shows that under simple road conditions, i.e. M1 road conditions, the optimal path is 29.809m. The optimal and worst solutions of both the traditional ACO path planning model and the improved ACO path planning model match the ideal path. This indicates that both path planning models can directly select the optimal path at this time. With the addition of U-shaped obstacles on the more intricate paths of M2 and M3, the optimal paths are 48.637 meters and 76.917 meters, respectively. The path planning model constructed through research can still accurately find the optimal path. However, traditional ACO path planning models can find the optimal solution under M2 road conditions, but meanwhile, they may also find poor paths. During M3 road conditions, the optimal solution was 77.503m, but it was not the optimal path, and the worst solution was 102.299m, resulting in severe deviation. This indicates that the improved ACO path planning model has strong environmental adaptability and can cope with path optimization problems in various complex environments.

Table 3. Overall results of simulation experiments.

Algorithm		M1	M2	M3
Optimal path length (m)		29.809	48.637	76.917
Optimal solution (m)	Traditional ant colony algorithm	29.809	48.637	77.503
	Improved ant colony algorithm	29.809	48.637	76.917
Worst-case solution (m)	Traditional ant colony algorithm	29.809	52.051	102.299
	Improved ant colony algorithm	29.809	48.637	76.917
Proportion of optimal solution	Traditional ant colony algorithm	100	100	100
	Improved ant colony algorithm	100	0	0

4.3. Comparative Experiment on Improving ACO Path Planning Model

To further verify the performance of the improved ACO path planning model, a comparative experiment was conducted between the ACO model and other intelligent optimization algorithms. The experimental objects include Genetic Algorithm (GA), PSO and Grey Wolf Optimizer (GWO). The study selected the environmental road conditions of M2 and brought four path planning models into the M2 environment for multiple iterations. Then, it collected data from multiple path planning results for comparison, and the convergence of the four path planning models is indicated in Figure 13.

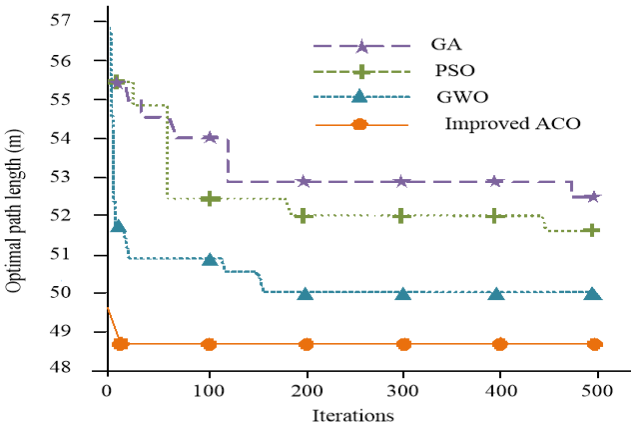

Figure 13. Convergence of four path planning models.

Figure 13 shows that the improved ACO path planning model exhibits faster convergence and finds shorter optimal paths than the other three models, while providing strong stability and optimal path guidance. It can significantly reduce the cost and time of unmanned target vehicle movement, and improve the training efficiency. The specific experimental data of the four path planning models are shown in Table 4.

Table 4 illustrates that in M2 road conditions, the GA path planning model generates an optimal path length of 52.973 meters. The PSO path planning model generates an optimal path length of 51.822 meters, whereas the GWO path planning model generates an optimal path length of 49.932 meters. And these three models all need to go through several iterations to stabilize the selection paths. The optimal path length planned by the improved ACO path planning model is 48.637m, and the turning point of the route is 6. Compared to other intelligent algorithms, this model has fewer turning points, smoother paths, and can quickly and stably plan routes, reducing collision rates. And it can accurately identify the optimal path, and the simulation experiment has proved that the improved ACO path planning model is suitable for path planning of unmanned target vehicles in complex environments.

Table 4. Specific experimental data of four path planning models.

Algorithm	GA	PSO	GWO	Improved ACO
Optimal path length (m)	52.873	51.822	49.932	48.637
Iterations	483	449	158	13
Number of inflection points	29	21	12	6

5. Conclusions

Traditional unmanned target vehicles are difficult to adapt to complex road conditions in complex situations and cannot achieve ideal military training results. Therefore, the study aims to improve the structure of the basic ACO algorithm and introduce the adjusted heuristic function into the ACO algorithm. Then, the combined GPS/BDS positioning system is explored and combined to design and plan the movement path of

unmanned target vehicles. The research results indicate that the robust adaptive positioning algorithm based on GPS/BDS pseudo range Doppler observation has smaller errors in three directions and higher positioning accuracy compared to the least squares method. The optimized positioning algorithm shows that the number of satellites has increased to 16, an increase of 6 compared to before optimization, and the average signal propagation time has decreased by 0.0001s. In large-scale positioning calculations, navigation accuracy can be significantly improved. In the ACO algorithm simulation experiment, under M3 road conditions, the improved ACO algorithm calculated the optimal distance of 76.917 meters, which is 0.586 meters less than the optimal distance calculated by the traditional ACO algorithm. This indicates that in challenging road conditions and U-shaped obstacles, the improved ACO algorithm can also consistently identify the optimal path, improving driving efficiency. Compared with other intelligent algorithms, the improved ant colony algorithm only iterates 13 times to calculate the optimal path length of 48.637. Both the number of iterations and the calculation results are much smaller than genetic algorithm, particle swarm optimization algorithm, and grey wolf optimization algorithm, indicating that the improved ACO algorithm has faster path planning speed and better smoothness. It also proves that the improved GPS/BDS positioning algorithm and the improved ACO algorithm designed in this study have the advantages of strong path planning ability and wide applicability. The algorithm holds significant utility in unmanned vehicle navigation and path planning. In the simulation experiments of the ACO algorithm, only U-shaped obstacles were considered, while in reality there are more complex terrains. Future research will further optimize the path planning methods and enhance the optimal path planning ability of the improved ACO path planning model in more complex road conditions.

Conflicts of interest

The authors report there are no competing interests to declare.

References

[1] Abdalla M., Mokhtar H., and Elgamal N., "HarmonyMoves: A Unified Prediction Approach for Moving Object Future Path," *International Journal of Advanced Computer Science and Applications*, vol. 11, no. 1, pp. 637-644, 2020. https://thesai.org/Downloads/Volume11No1/Paper_78-HarmonyMoves_A_Unified_Prediction_Approach.pdf

[2] Bao H., Du T., and Sun L., "Adaptive Attitude Determination of Bionic Polarization Integrated Navigation System Based on Reinforcement Learning Strategy," *Mathematical Foundations of Computing*, vol. 6, no. 2, pp. 161-177, 2023. Doi: 10.3934/mfc.2022014

[3] Boyineni S., Kavitha K., and Sreenivasulu M., "Mobile Sink-based Data Collection in Event-Driven Wireless Sensor Networks Using a Modified Ant Colony Optimization," *Physical Communication*, vol. 52, no. 6, pp. 10-23, 2022. https://doi.org/10.1016/j.phycom.2022.101600

[4] Che G., Liu L., and Yu Z., "An Improved Ant Colony Optimization Algorithm Based on Particle Swarm Optimization Algorithm for Path Planning of Autonomous Underwater Vehicle," *Journal of Ambient Intelligence and Humanized Computing*, vol. 11, no. 8, pp. 3349-3354, 2020. https://doi.org/10.1007/s12652-019-01531-8

[5] Chen H. and Zhang Y., "Dynamic Path Optimization in Sharing Mode to Relieve Urban Traffic Congestion," *Discrete Dynamics Nature and Society*, vol. 2021, no. 7, pp. 1-16, 2021. https://doi.org/10.1155/2021/8874957

[6] Cheng H., Liao W., Yang M., Rosenhahn B., and Sester M., "AMENet: Attentive Maps Encoder Network for Trajectory Prediction" *ISPRS Journal of Photogrammetry and Remote Sensing*, vol. 172, no. 3, pp. 253-266, 2021. https://doi.org/10.1016/j.isprsjprs.2020.12.004

[7] Cui Y., Ren J., and Zhang Y., "Path Planning Algorithm for Unmanned Surface Vehicle Based on Optimized Ant Colony Algorithm," *IEEJ Transactions on Electrical and Electronic Engineering*, vol. 17, no. 7, pp. 1027-1037, 2022. DOI: 10.1002/tee.23592

[8] Dey M., Das A., Banerjee A., Kamila U., and Chattopadhyay S., "Construction of Efficient Wireless Sensor Networks for Energy Minimization Using a Modified ACO Algorithm," *International Journal of Sensors Wireless Communications and Control*, vol. 11, no. 9, pp. 928-950, 2021. https://doi.org/10.2174/2210327911666210120122610

[9] Fang Y., Zhao W., Lin F., Wang D., and Wang J., "An AMC-Based Liquid Sensor Optimized by Particle-Ant Colony Optimization Algorithms," *IEEE Sensors Journal*, vol. 22, no. 3, pp. 2083-2090, 2022. DOI: 10.1109/JSEN.2021.3133688

[10] Fraser C. and Ulrich S., "Adaptive Extended Kalman Filtering Strategies for Spacecraft Formation Relative Navigation," *Acta Astronautica*, vol. 178, no. 1, pp. 700-721, 2021. https://doi.org/10.1016/j.actaastro.2020.10.016

[11] Gutmann S., Tstensen C., Bttcher I., Dietzel J., and Loderstedt S., "Clinical Use of a New Frameless Optical Neuronavigation System for Brain Biopsies: 10 Cases (2013–2020)," *Journal of Small Animal Practice*, vol. 63, no. 6, pp. 468-481, 2022. DOI: 10.1111/jsap.13482

[12] Hong J., Tu R., Zhang R., Fan L., and Zhang P., "Contribution Analysis of QZSS to Single-

Frequency PPP of GPS/BDS/GLONASS/Galileo," *Advances in Space Research*., vol. 65, no. 7, pp. 1803-1837, 2020. https://doi.org/10.1016/j.asr.2020.01.003

[13] Jao C. and Shkel A., "A Reconstruction Filter for Saturated Accelerometer Signals Due to Insufficient Far in Foot-Mounted Inertial Navigation System," *IEEE Sensors Journal*, vol. 22, no. 1, pp. 695-706, 2022. doi:10.1109/JSEN.2021

[14] Lin P., Yang J., Quan Y., and Chung C., "Potential Field-based Path Planning for Emergency Collision Avoidance with a Clothoid Curve in Waypoint Tracking," *Asian Journal of Control*, vol. 24, no. 3, pp. 1074-1087, 2022. https://doi.org/10.1002/asjc.2778

[15] Mahfoud S., Derouich A., Iqbal A., and Ouanjli N., "ANT-Colony Optimization-Direct Torque Control for a Doubly Fed Induction Motor: An Experimental Validation," *Energy Reports*, vol. 8, no. 10, pp. 81-98, 2022. https://doi.org/10.1016/j.egyr.2021.11.239

[16] Qian N., Gao J., Li Z., Fang C., and Pan C., "GPS/BDS Triple-Frequency Cycle Slip Detection and Repair Algorithm Based on Adaptive Detection Threshold and FNN-Derived Ionospheric Delay Compensation," *Acta Geodynamica et Geomaterialia*, vol. 17, no. 2, pp. 141-156, 2020. DOI: 10.13168/AGG.2020.0010

[17] Sathiya V., Chinnadurai M., and Ramabalan S., "Mobile Robot Path Planning Using Fuzzy Enhanced Improved Multi-Objective Particle Swarm Optimization," *Expert Systems with Applications*, vol. 198, no. 7, pp. 12-24, 2022. https://doi.org/10.1016/j.eswa.2022.116875

[18] Shi Y., Li J., Wang G., Bai S., and Bian G., "Establish Basic Reseach Funding Navigation System, Promote Technical Innovation to Underpin Development of National Modern Industrial System," *Bulletin of Chinese Academy of Sciences*, vol. 35, no. 5, pp. 573-579, 2022. https://doi.org/10.16418/j.issn.1000-3045.20210407007

[19] Tao L., Wu J., Ge D., Chen L., and Sun M., "Risk-Informed Based Comprehensive Path-Planning Method for Radioactive Materials Road Transportation," *Reliability Engineering and System Safety*, vol. 219, no. 3, pp. 6-12, 2022. https://doi.org/10.1016/j.ress.2021.108228

[20] Tian Y., Yuan L., Huang D., Zhou L., and Chen X., "Analysis of the Code and Phase Between-Receiver Inter-System Biases of the Overlapping Frequencies for GPS/Galileo/BDS," *Advances in Space Research*, vol. 65, no. 4, pp. 1196-1209, 2020. https://doi.org/10.1016/j.asr.2019.11.022

[21] Tu R., Zhang R., Liu Z., Fan L., and Han J., "Real-Time Detection of BDS Orbit Manoeuvres Based on the Combination of GPS and BDS Observations," *IET Radar, Sonar and Navigation*, vol. 14, no. 10, pp. 1603-1609, 2020. https://doi.org/10.1049/iet-rsn.2020.0171

[22] Wang E., Jia C., Qu P., Huang Y., and Jiang Y., "BDS/GPS Integrated Navigation Satellite Selection Algorithm Based on Chaos Particle Swarm Optimization," *Journal of Beijing University of Aeronautics and Astronautics*, vol. 45, no. 2, pp. 259-265, 2019. doi: 10.13700/j.bh.1001-5965.2018.0281

[23] Wu D., Zhu Z., Hu D., and Mansour R., "Optimizing Fresh Logistics Distribution Route Based on Improved Ant Colony Algorithm," *Computers, Materials and Continua*, vol. 000, no. 10, pp. 2079-2095, 2022. DOI:10.32604/cmc.2022.027794

[24] Xu S., "Research on Anomaly Detection Method for Hybrid Big Data Subarea Based on Ant Colony Algorithm," *International Journal of Information and Communication Technology*, vol. 17, no. 2, pp. 164-177, 2020. https://doi.org/10.1504/IJICT.2020.108965

[25] Xu T., Zhou H., Tan S., Li Z., and Ju X., "Mechanical Arm Obstacle Avoidance Path Planning Based on Improved Artificial Potential Field Method," *Industrial Robot*, vol. 49, no. 2, pp. 271-279, 2022. https://doi.org/10.1108/IR-06-2021-0120

[26] Zhang P., Tu R., Han J., Gao Y., Zhang R., and Lu X., "Characterization of Biases Between BDS-3 and BDS-2, GPS, Galileo and GLONASS Observations and Their Effect on Precise Time and Frequency Transfer," *Measurement Science and Technology*, vol. 32, no. 3, pp. 2-13, 2021. DOI:10.1088/1361-6501/abc963

Rongli Cai was born in Baoji, Shaanxi, China in 1974. He received the bachelor's degree from Taiyuan University of technology and a master's degree from Xi'an University of technology. At present, he works in the school of Optoelectronic Engineering of Xi'an University of technology. His research interests include optoelectronic testing, automatic control and embedded design.